

# Adaptive Pore Model for Fingerprint Pore Extraction \*

Qijun Zhao, Lei Zhang, David Zhang, Nan Luo  
Biometrics Research Centre, Department of Computing,  
The Hong Kong Polytechnic University, Kowloon, Hong Kong  
{csqjzhao, cslzhang, csdzhang, csnluo}@comp.polyu.edu.hk

Jing Bao  
Shenzhen Graduate School, Harbin Institute of Technology, China

## Abstract

Sweat pores have been recently employed for automated fingerprint recognition, in which the pores are usually extracted by using a computationally expensive skeletonization method or a unitary scale isotropic pore model. In this paper, however, we show that real pores are not always isotropic. To accurately and robustly extract pores, we propose an adaptive anisotropic pore model, whose parameters are adjusted adaptively according to the fingerprint ridge direction and period. The fingerprint image is partitioned into blocks and a local pore model is determined for each block. With the local pore model, a matched filter is used to extract the pores within each block. Experiments on a high resolution (1200dpi) fingerprint dataset are performed and the results demonstrate that the proposed pore model and pore extraction method can locate pores more accurately and robustly in comparison with other state-of-the-art pore extractors.

## 1. Introduction

Most existing automated fingerprint recognition systems (AFRS) utilize only level one and level two fingerprint features (e.g. orientation field and minutiae) for personal identification [5][6]. Level-three fingerprint features like pores, though seldom used by existing AFRS, are also very distinctive [8]. Thanks to the advancement of imaging techniques, more and more researchers [9][8][4][2][3] are now exploring how to

\*The work is partially supported by the CERF fund from the HKSAR Government, the central fund from Hong Kong Polytechnic University, the Natural Science Foundation of China (NSFC) under Contract No. 60620160097, and the National High-Tech Research and Development Plan of China (863) under Contract No. 2006AA01Z193 and 2007AA01Z195.

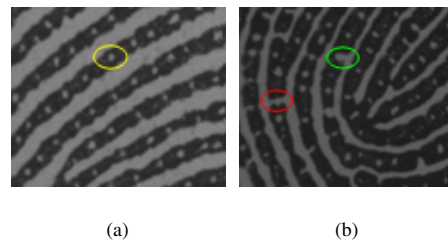
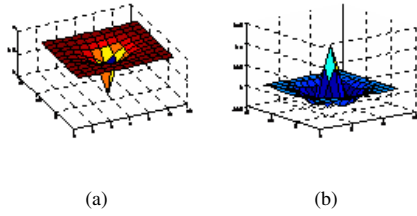


Figure 1. Partial fingerprints of two different fingers. (a) A closed pore and (b) two open pores are marked.

extract and use level-three features in AFRS. In [9], Stosz and Alyea presented, for the first time, an AFRS which uses both minutiae and pores to identify persons. Roddy and Stosz [8] statistically analyzed the individuality of pores on fingerprints and proved the power of pores in personal identification. Kryszczuk et al. [4] investigated the benefit of including pores in fragmentary fingerprint recognition and concluded that this benefit increases when the fragmentary fingerprint size decreases. Most recently, Jain et al. [2][3] proposed a high resolution AFRS using features from level 1 to level 3 (i.e. orientation fields, minutiae, pores and ridge contours).

A common challenge to the pore-based fingerprint recognition systems is how to accurately and robustly extract pores from fingerprint images. In this paper, we present an adaptive pore model based on our investigation in real pore profiles. The model can adjust its parameters adaptively according to the local ridge direction and period. A novel pore extraction method is then proposed based on this model.



**Figure 2. (a) Ray's and (b) Jain's pore models.**

## 2. Previous Work on Pore Extraction

Sweat pores reside on finger ridges, being either open or closed. An open pore is perspiring and appears on fingerprint images as a bright blob connected with the bright valley, whereas a closed pore appears as an isolated bright blob on the dark ridge (refer to Fig. 1). To the best of the authors' knowledge, the first pore extraction method, proposed by Stosz and Alyea [9], binarizes and skeletonizes the fingerprint image. A pore is detected once some criteria are met while tracking the skeleton. This skeletonization-based method was later used in [8][4]. As pointed out in [7][3], however, skeletonization is computationally expensive and very sensitive to noise. It can work well only on very high resolution fingerprint images, e.g. the fingerprint images used in [9][8][4] were at least 2000dpi.

Recently, Ray et al. [7] proposed an approach to extracting pores from 500 dpi fingerprint images using a pore model (refer to Fig. 2a), which is a slightly modified 2-dimensional Gaussian function:

$$M(i, j) = 1 - e^{-\sqrt{i^2+j^2}} \quad (1)$$

Pores are found by locating local areas that can match to the pore model with minimum squared errors. This method uses a filter of universal scale to detect pores. However, it is hard, even impossible, to find a universal scale suitable to all pores. Moreover, the pore model (1) is isotropic. This is not true for open pores, as we will show later.

Very recently, Jain et al. [2][3] proposed to use the following Mexican hat wavelet transform to extract pores based on their observation that pore regions typically have high negative frequency response as intensity values change abruptly from bright to dark at the pores:

$$w(s, a, b) = \frac{1}{\sqrt{s}} \int \int_{R^2} f(x, y) \phi\left(\frac{x-a}{s}, \frac{y-b}{s}\right) dx dy \quad (2)$$

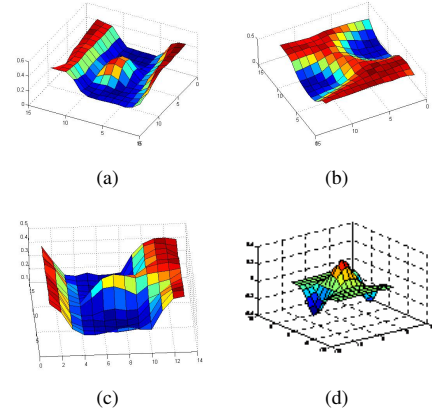


**Figure 3. (a)-(c) are three representative types of pore appearance, and (d) shows an example zero-degree adaptive pore model.**

The scale  $s$  in this pore model is experimentally set with a specific dataset. Fig. 2b shows the shape of the Mexican hat wavelet. Obviously, it is isotropic. This pore model is also limited by that the pore extractor cannot adapt itself to different fingerprints or different regions on a fingerprint.

In practical fingerprint recognition systems, either fingerprints of different fingers or fingerprints of the same finger could have ridges/valleys and pores of very different widths and sizes. Such problems become even worse when using high resolution fingerprint scanners. From the example fingerprint images shown in Fig. 1, one can easily see the variations in ridge/valley widths and pore sizes over different fingerprint images as well as across the same fingerprint. This motivates us to propose an adaptive pore model and the associated pore extraction method.

## 3. Adaptive Pore Modeling and Extraction

### 3.1. The Adaptive Pore Model

We manually marked and cropped hundreds of pores in several fingerprint images, including both open and closed pores. Based on the appearance of these real pores, we summarized three types of representative pore structures as shown in Fig. 3. Among them, the last two types correspond to open pores and they are not isotropic. With more observation of the pore appearance, we found that along the ridge direction, all the three types of pores appear with nearly Gaussian profile. Based on this, we propose the following pore model,

which is more accurate than previously presented ones [2][3][7],

$$APM_0(i, j) = e^{-\frac{j^2}{2\sigma^2}} \cdot \cos\left(\frac{\pi}{3\sigma}i\right) \quad (3)$$

$$APM_\theta(i, j) = Rot(APM_0, \theta) \quad (4)$$

where  $Rot(M, \theta)$  means rotating  $M$  by  $\theta$  degrees. The size of the pore model is set to  $6\sigma + 1$ , where  $\sigma$  is used to control the pore scale and it is determined by the local ridge period.  $\theta$  is used to control the direction of the pore model and it can be estimated by the local ridge orientation. Since both the two parameters are adaptively determined based on local fingerprint ridge period and orientation, we call this model the adaptive pore model (APM). Fig. 3d shows an example APM with  $\theta = 0$ .

### 3.2. The Pore Extraction Method

The proposed APM based pore extraction method includes three main steps. First, the fingerprint region is segmented from the fingerprint image (1200dpi) and the orientation field and ridge period are calculated. In order to reduce the computational cost and suppress noise, we down-sample the original fingerprint image to 600dpi and use the algorithms in [1] to calculate the ridge orientation and period. The obtained ridge orientation and period are then up-sampled to the original resolution. In this step, the binary ridge image is also obtained via thresholding the enhanced fingerprint image with the method in [1].

With the obtained ridge orientation field and period, we proceed to the pore extraction step. We partition the fingerprint image into blocks and extract pores block by block. For each block, we first calculate the ridge orientation inconsistency (OIC) defined as follows:

$$OIC(b) = std(\cos(2 \cdot O(b))) \quad (5)$$

where  $O(b)$  is the orientation field in the  $b^{th}$  block and  $std$  denotes the standard deviation. If the OIC of a block is less than a threshold (0.5 in our experiments) or the block size is very small (20 pixels in width and height),

we stop the partition; otherwise, we further averagely partition the block into four sub-blocks. We calculate the mean orientation  $\bar{\theta}$  and the median ridge period  $\hat{\tau}$  in the block and then set its local pore model as  $APM_{\bar{\theta}}$  with  $\sigma = \hat{\tau}/k$  ( $k = 12$  in our experiments). After obtaining the local APM, we take it as a matched filter and convolve it with the fingerprint image block. A threshold is then used to segment out the initial pores on the block.

The last step is to remove possible spurious pores. We apply the following constraints to post-processing the initial pore extraction results. (I) Pores should reside on ridges only. To implement this constraint, we use the binary ridge image as a mask to filter the extracted pores. (II) Pores should be within a range of valid sizes. We measure the size of a pore by counting the pixels in its region. (III) The mean intensity of a true pore should be large enough. In our experiments, we discarded the last 5% pores (i.e. those with lowest intensity). Finally, we record the extracted pores' locations as the coordinates of their mass centers.

## 4. Experiments and Discussion

Currently there is no public database of high resolution fingerprint images available. Therefore we built a 1200dpi fingerprint scanner and collected 198 fingerprint images ( $320 \times 240$ ). These fingerprints were taken from 33 index fingers, each of which has six samples taken in two sessions (about 5 days apart).

We manually marked the pores in ten fingerprint images. Fig. 4 shows a cropped fingerprint image, on which the pores are manually marked with brighter dots. The pore extraction results by the proposed APM based method, Ray's [7] and Jain's [2] methods are also shown in Fig. 4, where the extracted pores are marked with red circles. From Fig. 4, we can see that when the ridge widths change much, both Jain's and Ray's methods will miss some pores because they are not adaptive to the scale and orientation of pores and ridges. Instead, the proposed APM method can well adapt itself to local ridge width and orientation and it successfully detects

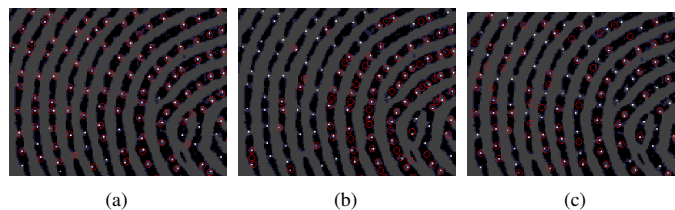
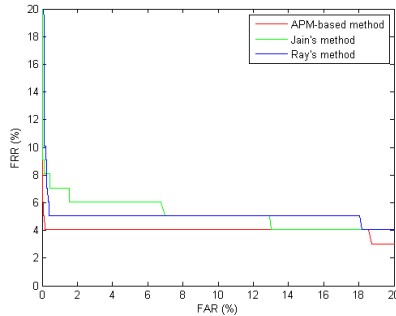


Figure 4. Pore extraction results by (a) APM based, (b) Jain's, and (c) Ray's methods.

**Table 1. True detection and false detection rates by the three methods.**

	APM-based	Jain's	Ray's
$R_T$	82.8%	74.1%	63.4%
$R_F$	13.9%	22.2%	20.4%



**Figure 5. The ROC curves by the three methods.**

most of the pores. The true detection rate  $R_T$  (i.e. the ratio of the number of detected true pores to the number of all true pores) and the false detection rate  $R_F$  (i.e. the ratio of the number of falsely detected pores to the number of all detected pores) were calculated on the ten fingerprint images for all the three methods. The average rates are listed in Table 1. The results show that the proposed method can extract pores more accurately and more robustly.

Furthermore, we assessed the contribution of the three pore extraction methods to the verification accuracy of AFRS. We implemented three simple AFRS. They use the same minutia extraction and matching methods, but are coupled with one of the three pore extraction methods respectively. The Iterative Closest Point (ICP) algorithm [3] is used to match the pores lying in the neighborhoods of two matched minutiae with higher similarity. The distance between two fingerprints is defined as the summation of three terms: the minutia based dissimilarity between them, the mean distance between matched pores (normalized to  $[0, 1]$ ), and the ratio of the number of unmatched pores to the total number of pores. Therefore, the differences between the verification accuracies of the three AFRS depend only on the pore extractors they use. The ROC curves by the three AFRS on our collected fingerprint image database are plotted in Fig. 5. These curves demonstrate again that the APM based method over-performs the other two

methods in contribution to verification accuracy. The EER of the APM based method is 4.04% whereas Jain's method 6.03% and Ray's method 5.05%.

## 5. Conclusions

This paper proposed an adaptive pore model (APM) based on the observation on real pore appearances. Different from existing pore models, the APM is anisotropic and it is adaptive to local fingerprint ridge direction and period. With the APM, a novel pore extraction method was then developed. A fingerprint image is partitioned into many blocks and pores are extracted block by block using locally defined APMs. The presented pore extraction method has been compared with some existing schemes by using 1200dpi fingerprint images. The experimental results demonstrate that the proposed APM and its associated pore extraction method can detect pores more accurately and robustly, and can help to improve the verification accuracy of pore based fingerprint recognition systems.

## References

- [1] L. Hong, Y. Wan, and A. Jain. Fingerprint image enhancement: Algorithms and performance evaluation. *IEEE Trans. Pattern Analysis and Machine Intelligence*, 20(8):777–789, 1998.
- [2] A. Jain, Y. Chen, and M. Demirkus. Pores and ridges: Fingerprint matching using level 3 features. *Proc. 18th International Conference on Pattern Recognition (ICPR'06)*, 4:477–480, 2006.
- [3] A. Jain, Y. Chen, and M. Demirkus. Pores and ridges: High-resolution fingerprint matching using level 3 features. *IEEE Trans. Pattern Analysis and Machine Intelligence*, 29(1):15–27, 2007.
- [4] K. Kryszczuk, A. Drygajlo, and P. Morier. Extraction of level 2 and level 3 features for fragmentary fingerprints. *Proc. Second COST Action 275 Workshop*, pages 83–88, 2004.
- [5] D. Maltoni, D. Maio, A. Jain, and S. Prabhakar. *Handbook of Fingerprint Recognition*. Springer, New York, 2003.
- [6] N. Ratha and R. Bolle. *Automatic Fingerprint Recognition Systems*. Springer, New York, 2004.
- [7] M. Ray, P. Meenen, and R. Adhami. A novel approach to fingerprint pore extraction. *Proc. Thirty-Seventh Southeastern Symposium on System Theory (SSST'05)*, pages 282–286, 2005.
- [8] A. Roddy and J. Stosz. Fingerprint features - statistical analysis and system performance estimates. *Proc. IEEE*, 85(9):1390–1421, 1997.
- [9] J. Stosz and L. Alyea. Automated system for fingerprint authentication using pores and ridge structure. *Proc. SPIE Conference on Automatic Systems for the Identification and Inspection of Humans*, 2277:210–223, 1994.